Simulation and Experimental Characterization of Compact Out-of-Plane Focusing Grating Couplers on 220 nm-SOI platform

(Student paper)

Hanna Becker [1], Clemens J. Krückel [2], Dries Van Thourhout [2], Martijn J.R. Heck [1]
[1]Department of Engineering, Aarhus University, Denmark
[2]Photonics Research Group, Department of Information Technology, Ghent University - imec
e-mail: hanna.becker@eng.au.dk

ABSTRACT

We present the design and characterization of compact out-of-plane focusing grating couplers on a silicon photonic platform, based on the fabrication restrictions for standard 193 nm UV lithography. The characterization by spatially sweeping a lensed fibre across the grating couplers clearly reveals the focusing behaviour and validates the design based on phase matching conditions for the one- and two-dimensional case. To our knowledge, this makes these grating couplers the first experimentally demonstrated 2D out-of-plane focusing grating couplers on a standard 220 nm-SOI platform. These grating couplers can find application as optical photonic layer couplers in optical sensing, as vertical interconnects, or to address spintronic memory elements.

Keywords: out-of-plane focusing grating couplers, photonic-electronic integration

1 INTRODUCTION

Grating couplers are key-components in the field of integrated photonics for fiber-to-chip coupling and continue to be actively investigated for various lab-on-chip technologies e.g., as demonstrated for fluorescence detection [1] or ion-trapping [2] applications. Furthermore, grating couplers have been utilized in phased arrays [3] for free-space beam forming and were proposed as optical photonic layer couplers (cf. Fig. 1 a) [4]. The footprint mismatch between photonics to electronics poses a major challenge for denser photonic-electronic integration, though requiring compact vertically focusing grating couplers (FGC). We designed compact out-of-plane FGC with the smallest footprint published so far. The structures presented here are of 5x5 µm and 10x10 µm respectively for the 1D and 2D components. The couplers were optimized with full 3D finite-difference time-domain (FDTD) simulations and their focusing characteristics are demonstrated experimentally.

The FGCs were specifically designed to address optically switchable spintronic memory elements, or more precisely magnetic random-access memory (MRAM) elements [5], [6]. The core component of spintronic memory, the magnetic tunnel junction (MTJ) will be illuminated by FGCs (cf. Fig.1 b). The binary state of the memory element will change if the optical energy absorbed in the all-optically switchable layer surpasses a material specific threshold value [7]. This makes efficient focusing and high peak intensities particularly important for this application.

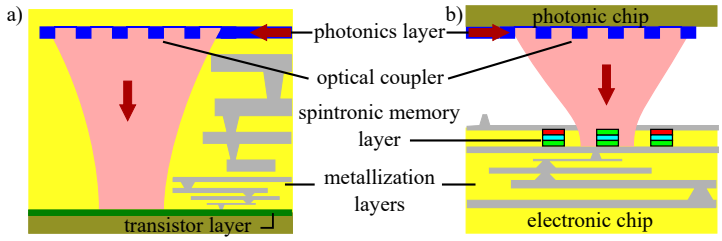

Figure 1. FGC as photonic layer couplers. a) FGC focuses light from photonic layer to logic layer. Schematic adapted from [4]. b) A photonic switch network addresses optically switchable spintronic memory elements via a focusing FGC.

2 DESIGN AND SIMULATION

The design of the 1D out-of-plane FGCs is based on the condition for constructive interference. For a chosen focal point at position (x_f, y_f, z_f), light propagating along the x-y-plane of the grating with effective index n_{eff} and the emitted light propagating in the cladding with refractive index n_{cl}, the interference condition becomes

$$n_{cl}\sqrt{x_f^2+y_f^2}+m_1\cdot\lambda_c=n_{\text{eff}}\sqrt{x^2+y^2}+n_{cl}\cdot\sqrt{(x_f-x)^2+(y_f-y)^2+z_f^2}. \quad (1)$$

Given light with the wavelength λ_c in vacuum and that $m_1 \in \mathbb{Z}$, this equation results in elliptically curved grating lines and a varying grating period along the grating [1]. The parameters from (1) are illustrated in Fig. 2 (a). Performed parameter sweeps of periodic gratings in 2D FDTD simulations map directionality and coupling angle against grating period and duty cycle, accounting for the restrictions provided by the use of a standard 220 nm-SOI platform and 193 nm UV lithography fabrication facilities. Based on these simulation-based look-up tables, the calculated period can be matched to the desired diffraction angle and grating strength for a given grating period. The numerically assembled gratings are simulated in a full 3D FDTD environment, using a commercial-grade FDTD program [8], and are further optimized by brute-force optimization techniques.

In a similar manner, the 2D polarization splitting grating couplers [9] are theoretically designed using the phase matching condition and then verified by 3D FDTD simulations. Since we are aiming to use the FGC as light emitters the 2D design offers additional advantages of polarization control [10] or polarization multiplexing schemes. To allow for polarization control, the grating is designed with two quasi TE inputs with a relative angle of 90 degrees to one another, one at the origin and one at a chosen coordinate $(x_2, y_2, 0)$ (cf. Fig. 2 (b)). Introducing a relative $\pm\pi/2$-phase shift of the inputs, will lead to a circularly polarized output. The phase matching condition is dictated by the following two conditions (I) and (II):

$$(I) \qquad n_{cl}\sqrt{x_f^2+y_f^2}+m_1\cdot\lambda_c = n_{\text{eff}}\sqrt{x^2+y^2}+n_{cl}\sqrt{(x_f-x)^2+(y_f-y)^2+z_f^2} \tag{2}$$

$$(II) \quad n_{cl}\sqrt{(x_f-x_2)^2+(y_f-y_2)^2}+m_2\cdot\lambda_c = n_{\text{eff}}\sqrt{(x-x_2)^2+(y-y_2)^2}+n_{cl}\sqrt{(x_f-x)^2+z_f^2+(y_f-y)^2} \tag{3}$$

Solutions meeting the conditions for m_1 and $m_2 \in \mathbb{Z}$ can be found numerically. The solutions are given by the intersections of the ellipses that meet the individual conditions. These diffraction centres can be etched as holes into the silicon slab waveguide.

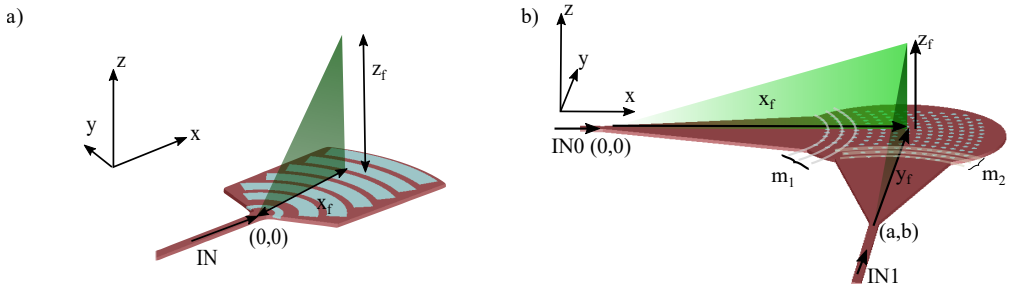

Figure 2. Schematic of the simulated FGCs. (a) Schematic of the 1D FGC and illustration of parameters used in (1). (b) Schematic of the 2D FGC and illustration of parameters used in (3).

3 EXPERIMENTAL EVALUATION OF THE FOCUSING CHARACTERISTICS

We applied the described design strategies to a multitude of FGCs with varying focal spot distances, ranging from 3 - 7 µm. The validity of the design approach is determined in a first step by evaluating the focusing characteristics of the fabricated gratings. To get an idea of the beam profile along the z-axis, orthogonal to the silicon photonic chip's surface, we mount a lensed fibre ($1/e^2$ spot size 2.5 µm) vertically above the chip on a motorized stage. A fibre starting position is chosen such that the fibre tip is as close as possible to the grating coupler yet still allowing contact-free movement above the chip. In a scan procedure, we move the fibre across the grating coupler in x- and and y-direction and evaluate the coupling efficiency $\eta(x,0)$ and $\eta(0,y)$. We calibrated the system in order to guarantee that each scan passes through the point with highest coupling efficiency. The fibre position above the chip is increased stepwise and the scan procedure is repeated for every vertical position. These profiles can be approximately fitted to the mode overlap integral η of an elliptical Gaussian mode profile E_{test} and the fibre mode E_{fibre}

$$\eta(x,y) = \frac{\int E_{fibre}(x,y)\cdot E_{test}^{*}\,\mathrm{d}A}{\int E_{fibre}^2(x,y)\,\mathrm{d}A\cdot\int E_{test}^{2^*}\mathrm{d}A}. \tag{4}$$

This allows us to extract approximate spatial dimensions of the beam profile from the measured traces. Exemplary results for a 1D FGC and a 2D FGC are depicted in Fig. 3 (a) and (b). Assuming a focused Gaussian beam profile, we expect to find the focal spot at the position where the coupling efficiency is maximum and the scanned cross-sections infers the narrowest beam dimension. The measurements show the expected behaviour and the focal spots are located at 3.5 µm and 4 µm above the grating. We

can deconvolve the measurements to find FWHM spot sizes of 3.9 µm^2 and 3.1 µm^2, respectively. This corresponds well to the average simulated focal spot of 3.3 µm^2.

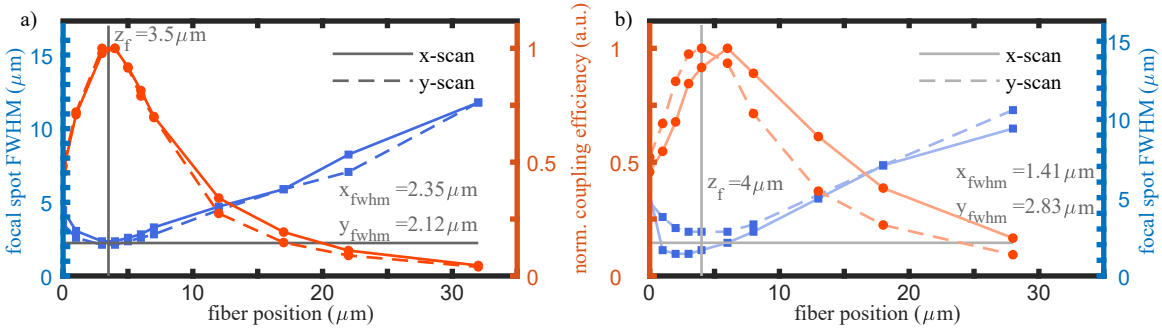

Figure 3. Exemplary measurement results from the spatial fibre cross-scan. (a) Extracted results from spatial scan for 1D FGC. X- and y-scan profiles converge towards a focus at a position of 3.5 µm. (b) Extracted results from spatial scan for 2D FGC. X- and y-scan profiles converge towards a median focus at a position of 4 µm.

4 CONCLUSION

The described design strategy results in out-of-plane FGCs. We experimentally determined the focussing characteristics by a spatial scan with a vertically mounted lensed fibre and evaluated the spatial dimension of the focus spot by fitting the scan traces with the mode-overlap integral (4). The measurements for the 1D FGC reveal a unique and well determined focal spot above the chip surface, estimating the FWHM in x- and y-direction of 2.3 µm and 2.1 µm and thus suggesting a rather uniformly shaped Gaussian beam profile. Experimental results for the 2D FGC also demonstrate the focusing character of the fabricated devices. The traces imply a slightly distorted focal spot with possible astigmatism. This demonstrates that purely relying on the phase matching conditions is adequate, but not entirely sufficient to produce a well-focused beam. Additional optimization routines during the design phase might lead to more precise focusing. Further effort will be put into determining the coupling efficiency, angular dispersion and bandwidth of the designs and thus deliver overall a better indicator for the performance of the designed grating couplers. Looking forward, the emission efficiency can be further improved considering fabrication processes that allow for stronger gratings like additional poly-silicon layers, multiple etch-depths and smaller feature sizes. The compact design yields a broad bandwidth and allows for the coupling of short pulses, needed for all-optical switching [10]. With improved designs likely exceeding coupling efficiencies of -3 dB, compact out-of-plane FGCs provide a suitable solution for photonic layer coupling and MTJ illumination in both heterogeneous or monolithic integration.

ACKNOWLEDGMENT

This project has received funding from the European Union's Horizon 2020 research and innovation programme under grant agreement No 713481.

REFERENCES

[1] S. Kerman et al., "Integrated Nanophotonic Excitation and Detection of Fluorescent Microparticles," ACS Photonics, vol. 4, no. 8, pp. 1937–1944, 2017.

[2] K. K. Mehta et al., "Integrated optical addressing of an ion qubit," Nat. Nanotechnol., vol. 11, no. 12, pp. 1066–1070, 2016.

[3] J. Sun, E. Timurdogan, A. Yaacobi, E. S. Hosseini, and M. R. Watts, "Large-scale nanophotonic phased array," Nature, vol. 493, no. 7431, pp. 195–9, 2013.

[4] D. Miller, "Attojoule Optoelectronics for Low-Energy Information Processing and Communications," J. Lightwave Technol. 35, 346-396 (2017).

[5] M. L. M. Lalieu, R. Lavrijsen, and B. Koopmans, "Integrating all-optical switching with spintronics," Nat. Commun., no. 2019, pp. 1–6.

[6] J. Chen, L. He, J. Wang, and M. Li, "All-Optical Switching of Magnetic Tunnel Junctions with Single Subpicosecond Laser Pulses," Phys. Rev. Appl., vol. 21001, pp. 2–7, 2017.

[7] M. Savoini et al., "Highly efficient all-optical switching of magnetization in GdFeCo microstructures by interference-enhanced absorption of light," Phys. Rev. B - Condens. Matter Mater. Phys., vol. 86, no. 14, pp. 1–5, 2012.

[8] Lumerical Inc. http://www.lumerical.com/tcad-products/fdtd/

[9] F. Van Laere et al., "Focusing Polarization Diversity Grating Couplers in Silicon-on-Insulator", Journal of Lightwave Technology, vol. 27, no. 5, pp. 612, 618, 2009.

[10] C. D. Stanciu et al., "All-optical magnetic recording with circularly polarized light," Phys. Rev. Lett., vol. 99, no. 4, pp. 1–4, 2007.